Inverse Problems **12** (1996) 869–883. Printed in the UK

Inverse conductivity problem for inaccurate measurements

Elena Cherkaeva and Alan C Tripp

The University of Utah, Department of Geophysics, 717 Browning Bldg, Salt Lake City, UT 84112, USA

Received 15 September 1995, in final form 8 May 1996

Abstract. In order to determine the conductivity of a body or of a region of the Earth using electrical prospecting, currents are injected on the surface, surface voltage responses are measured, and the data are inverted to a conductivity distribution. In the present paper a new approach to the inverse problem is considered for measurements containing noise in which data are optimally chosen using available *a priori* information at the time of the imaging. For inexact data the eigenvalues of the current-to-voltage boundary mapping show what part of the conductivity function can be confidently restored from the measurements. A special choice of measurements permits simple inversion algorithms reconstructing only this reliable part of the solution, hence reducing the dimension of the inverse problem. The inversion approach is illustrated in application to numerical modelling via a very fast approximate imaging solution.

1. Introduction

Traditional inversion of geo-electric surface data to a conductivity distribution presupposes that the strengths of the sources are predetermined by the geophysical practitioner and remain independent of the inversion process. The usual choice of uniform sources, which is logistically tractable, is appropriate if little *a priori* information is available about the conductivity structure. However, if significant *a priori* information concerning the geo-electric structure is known, as is the case in many geo-technical problems, then source strengths can be optimized as a function of the known conductivities, to maximize the resolution of the unknown component of the conductivity distribution. This optimization is discussed and is used as the foundation of an effective three-dimensional imaging algorithm.

The eigencurrents of the current-to-voltage boundary mapping give distributed transmitter currents which are ranked in information content by the size of the associated eigenvalues. Only a few dominant eigenvalues exceed the noise level of the data, and the corresponding eigencurrents are the only ones which give a voltage response above the data noise. A computationally efficient imaging algorithm can be developed for the measurements due to the dominant eigencurrents.

The present paper discusses one possible approach, in which injection currents, distributed over a set of discrete points, are optimized to maximize the resolution of a perturbation from some *a priori* conductivity distribution. The optimized injection currents are expanded in terms of the eigencurrents of the current-to-voltage boundary mapping, with the resolution of the conductivity distribution of the Earth dependent on the number of eigencurrents included in the expansion. The paper considers the implications of this expansion in the context of rapid and accurate imaging of geo-electric data. An algorithm using data of only one eigencurrent is developed based on this approach; this algorithm is applied to a numerical example for a conductive perturbation about a resistive body.

0266-5611/96/060869+15$19.50 © 1996 IOP Publishing Ltd

2. Formulation of the inverse problem

Let Ω be a domain filled with a material of known, not necessary spatially constant, conductivity γ, with some unknown inclusions of conductivity $\gamma + \sigma$, where σ can also vary spatially. We can apply various currents f on the boundary of the domain $\partial\Omega$ and measure the corresponding voltage responses due to the applied excitations.

We consider the problem with the function γ as a background problem, the corresponding solutions of which are known. The problem is to find the unknown function of conductivity σ.

The potentials and currents for the background medium γ and the real medium $\gamma + \sigma$ satisfy the conductivity equations

$$\nabla(\gamma + \sigma)\nabla w = 0 \qquad \text{in } \Omega \qquad (\gamma + \sigma)\frac{\partial w}{\partial n} = f \qquad \text{on } \partial\Omega \tag{1}$$

and

$$\nabla\gamma\nabla u = 0 \qquad \text{in } \Omega \qquad \gamma\frac{\partial u}{\partial n} = f \qquad \text{on } \partial\Omega \tag{2}$$

where the current f satisfies the integral zero restriction:

$$\int_{\partial\Omega} f \, \mathrm{d}x = 0. \tag{3}$$

Solution of the equation (1) is unique up to a constant component which is determined if a zero value of the function is prescribed; so we assume that $\int_{\partial\Omega} u \, \mathrm{d}x = 0$ and $\int_{\partial\Omega} w \, \mathrm{d}x = 0$.

In the inverse problem we want to determine the function σ from the knowledge of potential responses $w \,|_{\partial\Omega}$ measured on the boundary $\partial\Omega$. The solution of this problem is unique in the class of smooth or piecewise analytic functions [9, 15, 20] provided the Neumann-to-Dirichlet maps $R_{\gamma+\sigma}$ and R_γ are known:

$$R_{\gamma+\sigma}(f) = w|_{\partial\Omega} \qquad w \in (1) \qquad \text{and} \qquad R_\gamma(f) = u|_{\partial\Omega} \qquad u \in (2). \tag{4}$$

Assuming that the conductivity perturbation is small let us linearize the equations with respect to the conductivity perturbation. The linearized equation for small σ is an equation for the additional scattering potential $v = w - u$, and can be obtained from equations (1) and (2). We assume that $\mathrm{supp}(\sigma) \in \tilde{\Omega}$ for some subdomain $\tilde{\Omega} \subset \Omega$, and $\sigma(x) = 0$, for $x \in \Omega \setminus \tilde{\Omega}$. We suppose that $\sigma \in L^2(\tilde{\Omega})$. Then

$$\begin{aligned} &\nabla \cdot \gamma\nabla u = 0 \qquad \text{in } \Omega \qquad \gamma\frac{\partial u}{\partial n} = f \qquad \text{on } \partial\Omega \\ &\nabla\gamma\nabla v = -\nabla\sigma\nabla u \qquad \text{in } \Omega \qquad \gamma\frac{\partial v}{\partial n} = 0 \qquad \text{on } \partial\Omega. \end{aligned} \tag{5}$$

Here f is an applied current, u is a potential of the electrical field in the model background problem, and v is a fluctuation of the potential caused by the presence of the inclusion.

The inverse linearized problem is to find a conductivity distribution σ which fits the measured potential difference v satisfying (5) on the surface for the different currents f.

Using Green's second formula the solution of the system (5) can be represented in integral form. From the second equation the function v is expressed as

$$\begin{aligned} v(x) &= \int_\Omega \nabla\sigma\nabla u(y) G(x, y) \, \mathrm{d}y \\ &= -\int_\Omega \sigma(y)\nabla_y u(y)\nabla_y G(x, y) \, \mathrm{d}y. \end{aligned} \tag{6}$$

Here $G(x, y)$ is the Green's function for the model background problem.

Analogously, function u is presented as

$$u(y) = \int_{\partial\Omega} f(z)G(y, z)\,\mathrm{d}z. \tag{7}$$

Substitution of the last expression into (6) and differentiation by parts gives:

$$v(x) = -\int_{\Omega} \sigma(y) \int_{\partial\Omega} f(z)\nabla_y G(z, y)\nabla_y G(x, y)\,\mathrm{d}z\,\mathrm{d}y. \tag{8}$$

This is a linear integral operator usually exploited when solving an inverse problem. When σ is expanded in a finite series in terms of given functions (for example, such as piecewise constant functions) with unknown coefficients σ_n, (8) gives an explicit expression for the Jacobian matrix which needs to be inverted. Solution of the integral equation (8) gives the formal solution to the inverse problem given f.

Different inversion schemes have been developed in application to inverse electrical tomography, nondestructive testing, and the inverse geo-electrical problem; see for example a description of inversion techniques applied to the resistivity inverse problem [16] in geophysics. Most of them deal with data as given, constructing methods of solution which fit all the data. Recently a new approach has been taken which selects the data to use. A very effective algorithm was suggested and numerically tested in [3, 19] for determination of linear crack location by electrical measurements. The paper [8] contains a detailed discussion of inverse problem resolution based on usage of different data sets.

In the present paper we suggest a solution of the linearized inverse problem for noisy measurements. Only a part of the conductivity function can be confidently reconstructed from noisy measurements. The eigenvalues of an operator mapping the injected currents to the voltage response difference measured on the boundary show what part of the solution can be restored. Reconstruction of this part of the solution permits simplification of an imaging algorithm. In the next sections we discuss how a special choice of the functions f can simplify the inversion procedure.

3. The optimal currents

Currents applied on the boundary generate different voltage responses for the background and the real media. Those which give the greatest anomalous response will be appropriate for solving (8). In [13] currents with unit L_2 norm on the boundary, which maximize the voltage difference, were considered in connection with the problem of distinguishability of an inclusion. In [4] examples are given of the currents which maximize the anomalous response for three-dimensional models in a geoelectrical context.

Let us formulate the problem to which these currents provide the solution. Again let $R_\gamma(f)$ be the voltage response $u|_{\partial\Omega}$ on the boundary of the medium γ due to an applied current f. Thus the boundary value of a function v which solves the equation (5) equals the function $R_{\gamma+\sigma}(f) - R_\gamma(f)$ for the applied current f.

Then the problem of maximizing the response on the boundary is an optimization problem with respect to the current:

$$M = \max_{f\in\mathcal{F}} \|R_{\gamma+\sigma}(f) - R_\gamma(f)\|_{L_2(\partial\Omega)} \tag{9}$$

where $\mathcal{F}$ is a chosen set of functions. Since the voltages are linear with f, we must restrict the intensity of the injected current to avoid infinite values in the maximization procedure. As in [13, 10] we fix the $L_2(\partial\Omega)$ norm of the applied currents

$$\mathcal{F} = \{f : \|f\|_{L_2(\partial\Omega)} = 1\}. \tag{10}$$

With this restriction the problem (9) is an eigenvalue problem and its solution can be found numerically using a standard SVD technique applied to the matrix of responses [4, 5] or with adaptively changing injection current patterns [10] as an implementation of the power method.

Solution of the problem (9) is a system of monotonically decreasing eigenvalues $\{M_i\}$ with the corresponding orthogonal eigenfunctions $\{f_i\}$, $i = 1, 2, \ldots$.

Being a solution of an eigenvalue problem the eigenfunction $f_1 \in \mathcal{F}$ maximizing the functional (9) for the linearized problem (5) is proportional to the values of the function $v_1 = R_{\gamma+\sigma}(f_1) - R_\gamma(f_1)$ on the boundary,

$$f_1(x) = \frac{1}{\mathcal{M}_1} v_1(x) \qquad x \in \partial\Omega \qquad \text{with } \mathcal{M}_1^2 = M_1^2 = \int_{\partial\Omega} v_1^2 \, \mathrm{d}x \tag{11}$$

where the sign of constant $\mathcal{M}_1$ depends on the sign of the perturbation from the background conductivity σ, and M_1 is the first eigenvalue of the problem (9).

A relationship similar to (11) is valid for every eigenfunction. Hence for any i the eigencurrent and the corresponding potential satisfy the system of equations:

$$\begin{aligned} &\nabla\gamma\nabla u_i = 0 \qquad \text{in } \Omega \qquad \gamma\frac{\partial u_i}{\partial n} = f_i = \frac{1}{\mathcal{M}_i} v_i \qquad \text{on } \partial\Omega \\ &\nabla\gamma\nabla v_i = -\nabla\sigma\nabla u_i \qquad \text{in } \Omega \qquad \gamma\frac{\partial v_i}{\partial n} = 0 \qquad \text{on } \partial\Omega \end{aligned} \tag{12}$$

Utilizing this property of the eigenfunctions an integral representation for the eigencurrent can be derived as follows. From the expression (8) we have an integral equation for the eigenfunctions solving the eigenvalue problem (12):

$$f_i(x) = -\frac{1}{\mathcal{M}_i} \int_{\partial\Omega} f_i(z) \int_\Omega \sigma(y) \nabla_y G(z, y) \nabla_y G(x, y) \, \mathrm{d}y \, \mathrm{d}z. \tag{13}$$

The eigenvalue $\mathcal{M}_i$ of the spectral problem (12) is

$$\mathcal{M}_i = \int_{\partial\Omega} f_i(x) v_i(x) \, \mathrm{d}x. \tag{14}$$

Hence the result of multiplication of the expression (13) by $v_i(x)$ and integration over $\partial\Omega$ shows that the eigenvalues $\mathcal{M}_i$ are the scalar products of the function σ with some functions in $L^2(\Omega)$.

$$\mathcal{M}_i = -\int_\Omega \sigma(y) \nabla u_i(y) \nabla u_i(y) \, \mathrm{d}y = -(\sigma, |\nabla u_i|^2)_{L^2(\Omega)}. \tag{15}$$

The functions ∇u_i are electric fields in the background medium generated by the applied currents f_i.

Similarly it follows from the orthogonality property of the eigenfunctions f_i that the projection of σ on the directions corresponding to the functions which are pointwise scalar products $\nabla u_i(y) \nabla u_j(y)$, $y \in \Omega$, between the electric fields ∇u_i and ∇u_j generated by different eigencurrents f_i and f_j is zero.

$$\int_{\partial\Omega} f_i(z) v_j(z) \, \mathrm{d}z = \int_\Omega \sigma(y) \nabla u_i(y) \nabla u_j(y) \, \mathrm{d}y = 0. \tag{16}$$

4. Equivalency of inverse solutions for inaccurate measurements

It is well known that the resolution of the inverse conductivity problem is not very high [1, 7, 14, 17]. In this section we show that the solution of the inverse problem for a data set containing noise and the solution corresponding to the data set generated by only a few dominant eigencurrents are equivalent solutions. The number of these eigencurrents is determined by the data noise level, and of course, it depends on the difference between the real and the background conductivity distributions.

We apply the SVD technique to the impedance difference matrix, which immediately gives us information about linear combinations of our data—which are valuable, and which are not. Figure 2 in section 7 shows an example of such an analysis for the simulated model. One can see that only a few dominant eigenvalues are significant. In this section we show that if instead of all data we consider only data generated by the eigencurrents corresponding to these eigenvalues, we are not able to distinguish the inversion results.

The eigenvalues $\{M_i\}$ form a sequence of rapidly decreasing values [10]. It is clear that only data from currents with eigenvalues which are greater than the noise level in the measurements contain valuable information about the conductivity distribution. Numerical results of computing the eigenvalues for the models used in [5] show that only two to five eigenvalues are greater than the reasonable noise in measurements.

Suppose that noise of a level ϵ is present in the data such that starting from some M_m

$$M_k < \epsilon \qquad k > m. \tag{17}$$

This means that the potential difference due to the currents $f_k, k > m$, registered on the boundary $\partial\Omega$ cannot be distinguished from the noise level:

$$M_k = \|R_{\gamma+\sigma}(f_k) - R_\gamma(f_k)\|_{L_2(\partial\Omega)} < \epsilon. \tag{18}$$

In this case without loss of accuracy, we can set $M_k, k > m$ to be equal to zero. Different solutions σ_1 and σ_2 of the inverse problem for two sets of measured potential differences $\{v_1, v_2, \ldots, v_m, v_{m+1}, \ldots\}$ and $\{v_1, v_2, \ldots, v_m, 0, 0, \ldots\}$ should be recognized as equivalent solutions.

Indeed, let σ_1 be a true solution of the inverse problem:

$$R_{\gamma+\sigma_1}(f_i) - R_\gamma(f_i) = v_i \qquad i = 1, 2, \ldots \tag{19}$$

and σ_2 be a solution satisfying a 'cut' system of restrictions:

$$R_{\gamma+\sigma_2}(f_i) - R_\gamma(f_i) = \begin{cases} v_i & i = 1, 2, \ldots, m \\ 0 & i > m. \end{cases} \tag{20}$$

The eigenfunctions $\{f_i\}$ form an orthonormal complete system in $\hat{L}_2(\partial\Omega) = \{f : f \in L_2(\partial\Omega), \int_{L_2(\partial\Omega)} f \, \mathrm{d}x = 0\}$. Hence any applied current f is presented as

$$f = \sum \alpha_i f_i \qquad \sum \alpha_i^2 = 1 \tag{21}$$

and the corresponding potential difference measured on the surface is

$$R_{\gamma+\sigma_1}(f) - R_\gamma(f) = \sum_{i=1}^{\infty} \alpha_i M_i f_i \qquad R_{\gamma+\sigma_2}(f) - R_\gamma(f) = \sum_{i=1}^{m} \alpha_i M_i f_i \tag{22}$$

Then for any applied current the difference between the potential values on the surface generated by the functions $\gamma + \sigma_1$ and $\gamma + \sigma_2$ is less than the error of measurements

$$\max_{f \in \hat{L}_2(\partial\Omega), \|f\|=1} \|R_{\gamma+\sigma_1}(f) - R_{\gamma+\sigma_2}(f)\|_{L_2(\partial\Omega)} = M_{m+1} < \epsilon \tag{23}$$

and no current applied on the boundary can generate a noticeable difference, i.e. the systems of equations (19) and (20) give equivalent solutions. In what follows, we consider the inverse of the more appropriate set, (20), and assume that

$$M_1 > M_2 > \cdots > M_m > \epsilon \qquad M_{m+1} = M_{m+2} = \ldots = 0. \tag{24}$$

In the part of the paper describing numerical simulations we consider a case when only the first eigenvalue is not zero:

$$M_1 \neq 0 \qquad M_2 = M_3 = \ldots = 0. \tag{25}$$

5. Inversion

Using only a finite number of currents we cannot hope to reconstruct the unknown distribution of conductivity uniquely even for noise-free measurements. However, we would like to ensure uniqueness of the numerical construction of the solution. Therefore we take a minimal norm solution obtained using a variational approach similarly to [8]. We obtain a moment problem [1, 6, 18] for the data corresponding to the dominant eigencurrents. Since the system of equations has a special form, we can develop a solution in a simple fashion.

We will show first that a minimal norm solution of the inverse problem has a form

$$\sigma(y) = \sum_{i,j} \lambda_{i,j} \nabla u_i(y) \nabla u_j(y) \qquad y \in \tilde{\Omega} \tag{26}$$

where u_i is a solution of the problem for an applied current f_i and $\lambda_{i,j}$ are some constants.

Let us suppose that we have applied N different eigencurrents on the surface $\partial\Omega$ and measured the corresponding voltage responses.

We want to find a function σ which is of minimal norm, and which provides eigenvalues of the currents-to-data map $M_i(\sigma)$, $i = 1, 2, \ldots, N$, equal to the eigenvalues M_i obtained from measurements. In addition the function σ should generate orthogonal responses v_i and v_j for different optimal currents f_i and f_j. In short the function σ should satisfy equations (15) and (16).

The function σ should produce the voltage response $R_{\gamma+\sigma}(f_k) - R_\gamma(f_k)$, which can be expanded in terms of the orthogonal system of functions $\{f_i\}$ with the coefficients of the expansion equal to:

$$((R_{\gamma+\sigma}(f_k) - R_\gamma(f_k)), f_j) = b_{i,j} \tag{27}$$

where $b_{i,j}$ are the indexed integrals in (15) and (16), $i = 1, 2, \ldots, N$, $j = 1, 2, \ldots, N$. In general $b_{i,i} = -\mathcal{M}_i$ and $b_{i,j} = 0$ for $i \neq j$. Thus instead of matching the measured responses, we try to fit their orthogonal expansions. The equations (15) and (16) then assume the form:

$$\int_\Omega \sigma(y) \nabla u_i(y) \nabla u_j(y)\, \mathrm{d}y = b_{i,j} \qquad i = 1, 2, \ldots, N \qquad j = 1, 2, \ldots, N. \tag{28}$$

We take as a variational functional the norm of the solution σ:

$$J = \min_{\sigma \in \mathcal{R}} \|\sigma\|^2_{L^2(\Omega)}. \tag{29}$$

The constraint set $\mathcal{R}$ is the set of conductivity distributions satisfying the equations (28).

We bring these constraints into an augmented functional $\tilde{J}$ with Lagrange multipliers $\lambda_{i,j}$.

$$\tilde{J} = \min_\sigma \int_\Omega \sigma^2(y)\, \mathrm{d}y + \sum_{i,j} \lambda_{i,j} \left(\int_\Omega \sigma(y) \nabla u_i(y) \nabla u_j(y)\, \mathrm{d}y - b_{i,j} \right) \tag{30}$$

where the indices of summation i and j run from 1 to N.

The optimal solution satisfies the Euler equation which is obtained from the functional (30) by varying σ. Thus a necessary condition of optimality gives an expression for the unknown σ:

$$\sigma(y) = \sum_{i,j} \lambda_{i,j} \nabla u_i(y) \nabla u_j(y) \qquad y \in \tilde{\Omega}. \tag{31}$$

Here u_i and u_j are the solutions of the problem for the applied eigencurrents f_i and f_j.

The coefficients $\lambda_{i,j}$ can now be found from equations (28).

Simplifying notation, we denote $\nabla u_i \nabla u_j$ as functions g_k, $k = 1, 2, \ldots, N^2$ in $L^2(\Omega)$ with the scalar product

$$(g_k, g_l) = \int_\Omega g_k(y) g_l(y)\, \mathrm{d}y. \tag{32}$$

Equation (31) then implies that we are seeking a function σ in a subspace S of $L^2(\Omega)$ spanned by the vectors g_k:

$$S = \mathrm{Span}\{g_1, g_2, g_3, \ldots, g_K\} \qquad K = N^2 \tag{33}$$

and

$$\sigma = \sum_{k=1}^{K} \alpha_k g_k \tag{34}$$

where scalar coefficients α_k are the coefficients $\lambda_{i,j}$, $i = 1, \ldots, N$, $j = 1, \ldots, N$.

The direct approach is to use the expression (34) and relationships (28) to determine the coefficients α_k via a 'method of moments' approach (see, e.g., [11]). Hence we form the Gramian G for the functions $\{g_k\}$

$$G(g_1, g_2, \ldots, g_K) = \begin{bmatrix} (g_1, g_1) & \ldots & (g_1, g_K) \\ (g_2, g_1) & \ldots & (g_2, g_K) \\ \ldots & \ldots & \ldots \\ (g_K, g_1) & \ldots & (g_K, g_K) \end{bmatrix} \tag{35}$$

and we face the problem of solving the linear system obtained from (28)

$$GX = B \qquad X = [\alpha_1, \ldots, \alpha_K]^T \qquad B = [b_{1,1}, b_{1,2}, \ldots, b_{N,N}]^T \tag{36}$$

which is ill-posed.

An effective way of solving the problem follows from analysis of the relationships (15), (16) and (24) which show that the projections of the function σ on the functions $g_k = \nabla u_i \nabla u_j$ are different from zero only when $i = j$, $i < m$. Let the set of such indices k be Z_1, and the set of the indices k of the functions g_k with zero scalar product with σ be Z_2, and $Z_1 + Z_2 = \{1, 2, \ldots, K\}$.

From (15), (16) and (24) it follows that the function σ is $L^2(\Omega)$ orthogonal to any function g_k, $k \in Z_2$:

$$\sigma(y) = \alpha\phi(y) \qquad \phi \perp g_k \qquad k \in Z_2 \tag{37}$$

where α is a scalar.

This means that the function σ lies in the subspace T_1 of S which is orthogonal to the subspace T_2 spanned by the vectors g_k, $k \in Z_2$.

$$T_2 = \mathrm{Span}\{g_{k_1}, g_{k_2}, \ldots, g_{k_{K-m}}\} \qquad k_i \in Z_2 \qquad T_1 \cup T_2 = S. \tag{38}$$

Hence what we need to do in order to find the function σ is to compute a subspace T_1 of S which is orthogonal to the subspace $T_2 = \mathrm{Span}\{g_{k_i}, k_i \in Z_2\}$ and contains the solution $T_1 = S \backslash T_2$, and then to solve for σ in the subspace T_1 of dimension m instead of K.

Let us for simplicity consider the case when $m = 1$, so that only one current generates data which are significantly greater than the noise level. The sets Z_1 and Z_2 in this case are $\{1\}$ and $\{2, 3, \ldots, K\}$, and in order to find the function σ we need to calculate a direction ϕ in S which is orthogonal to the subspace $T_2 = \text{Span}\{g_2, g_3, \ldots, g_K\}$.

$$\phi \in S \qquad \phi \perp g \qquad \forall g \in T_2. \tag{39}$$

Then we use the length of the non-zero projection (15) of σ on g_1 to calculate the scalar coefficient α:

$$\alpha = -\mathcal{M}_1/(g_1, \phi). \tag{40}$$

Hence we orthogonalize the system of functions $\{g_k\}$, $k = 2, 3, \ldots, K$ and get an orthonormal system $\{\phi_i\}$, $i = 1, 2, \ldots, K-1$ which provides a basis in the subspace T_2. The function ϕ which satisfies (39) is then obtained as

$$\phi = g_1 - \sum_{i=1}^{K-1} (g_1, \phi_i)\phi_i \tag{41}$$

and the coefficient α is found from (40).

In a general case when $m > 1$ we still have to solve a linear system to calculate σ, but its dimension m is much less than the dimension of the original system K.

6. Analysis of the numerical algorithm

Now we discuss numerical implementations of the suggested approach and in the next section we describe the results of computer simulations.

We need to mention that solving for σ in the subspace T_1 of the dimension m instead of the space S of the original dimension K does not decrease the accuracy of calculations. As a solution we obtain a conductivity function which is equivalent up to the noise level to the true solution.

A less time consuming way is possible when subspace T_1, which is the complementary subspace to T_2 and contains the solution, and T_2 are well separated. In this case, the scalar products of the functions (g_{k_i}, g_{k_j}), $k_i \in Z_1$, $k_j \in Z_2$ are close to zero.

As the function σ is orthogonal to any function g_{k_j}, $k_j \in Z_2$ and the scalar products of the functions (g_{k_i}, g_{k_j}), $k_i \in Z_1$, $k_j \in Z_2$ are negligible in this case, the coefficients α_{k_j} of the expansion (34) are zero for $k_j \in Z_2$. Then

$$\sigma = \sum_{k_i \in Z_1} \alpha_{k_i} g_{k_i} \tag{42}$$

and we only need to solve the system of equations with the matrix of dimension m of the scalar products of the functions $\{g_{k_i}, k_i \in Z_1\}$.

When $m = 1$, this corresponds to the situation that the function g_1 is taken as an approximation of ϕ. This is the way we proceed in the numerical simulations, results of which are described in the next section.

Using (15) we find the coefficient of proportionality α is expressed via a norm of the background field:

$$\alpha = -\frac{\mathcal{M}_1}{\||\nabla u_1|^2\|^2}. \tag{43}$$

The final expression for the approximate minimal norm solution for one current data is:

$$\sigma(y) = -\frac{\mathcal{M}_1}{\||\nabla u_1|^2\|^2} |\nabla u_1(y)|^2 \tag{44}$$

with the norm $||\sigma||$ equal to $M_1/\|\|\nabla u_1|^2\|$. Here M_1 is the first eigenvalue of the eigenvalue problem (9) and $\mathcal{M}_1$ is the first eigenvalue of the eigenvalue problem (12).

There is an assumption in the formulation of the problem that we need to confront. We assume that the inclusion is located at some distance from the boundary. As pictures in [5, 4] show, the optimal current distribution inside the body concentrates near the surface electrodes and in the region of the inhomogeneity. The behaviour of the optimal electrical field is similar. Therefore, if we do not eliminate in advance the influence of the surface electrodes it leads to a numerical algorithm which can be unstable—the first step of the iteration reveals a big 'false' inclusion near the boundary, then the second step needs to take it out, and so on. In order to avoid this, at least in such cases when we have additional information about the approximate depth of the inclusion, we can introduce a weight function $q(y),\ y \in \Omega$, which attenuates the field near the electrodes. For example, if we know that the inclusion is located not closer to the surface than h we can take a unit weight function for the depths greater than h and let it grow exponentially when approaching the boundary.

In this case instead of functional (30) we need to consider the following functional J_q:

$$J_q = \min_{\sigma \in \mathcal{R}} \|\sigma\|^2_{L_2(\Omega;q)} \tag{45}$$

with the same restrictions (28). The corresponding augmented functional $\tilde{J}_q$ is:

$$\tilde{J}_q = \min_{\sigma} \int_\Omega q(y)\sigma^2(y)\,\mathrm{d}y + \sum_{i,j} \lambda_{i,j} \left(\int_\Omega \sigma(y) \nabla u_i(y) \nabla u_j(y)\,\mathrm{d}y - b_{i,j} \right). \tag{46}$$

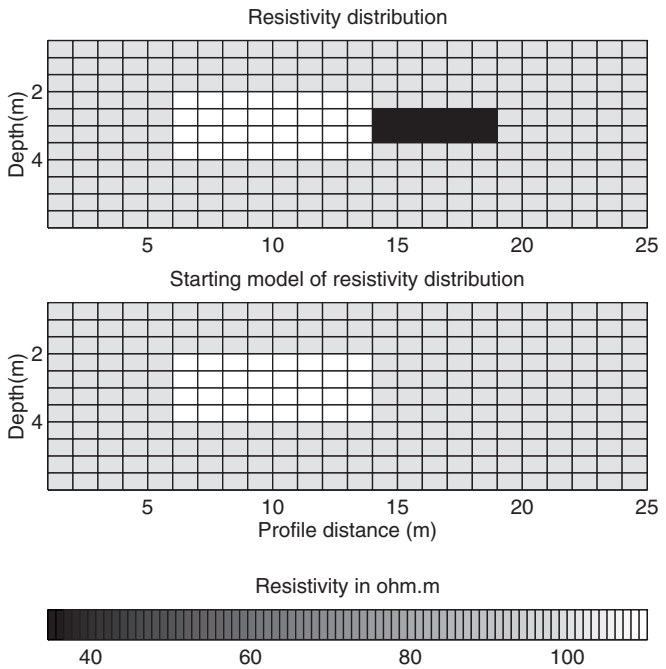

Figure 1. Cross section of the real medium with leak (top) and the starting model (bottom). The scale on the bottom shows the values of resistivity in $\Omega\ \mathrm{m}^{-1}$.

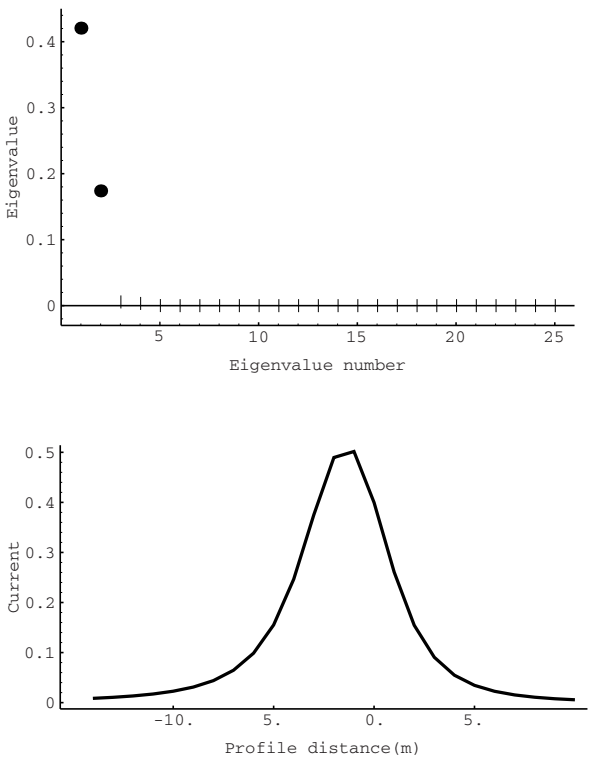

Figure 2. Distribution of eigenvalues M_i before starting the inversion (top) and the intensity distribution of the first optimal current (bottom).

The optimal solution of this problem is obtained analogously by varying σ:

$$\sigma(y) = \sum_{i,j} \lambda_{i,j} \frac{\nabla u_i(y) \nabla u_j(y)}{q(y)}. \tag{47}$$

7. Results of computer simulations

In numerical simulations we assume the case where the relationship between the data noise and the eigenvalues of the current-to-voltage mapping is such that only the first eigenvalue M_1 can be considered to be significantly greater than zero. In this case only the data set corresponding to the first optimal current contains important information about an inclusion. We show numerical results of iterative use of the algorithm of approximating the solution for one injected current. The application is numerically modelling a geo-environmental problem of monitoring a contaminated area.

We apply the developed algorithm to the following problem of monitoring a contaminated area. Let us consider a region of the Earth containing a waste deposit which can leak. We assume that the waste container is resistive, and that the probable leakage is conductive. Thus the model background resistivity distribution consists of a homogeneous Earth material of resistivity 100 Ω m^{-1} with an embedded container of resistivity 1000 Ω m^{-1}. The size of the container is 5 m by 2 m by 1 m. We assume that the container leaks, and we take as the real medium the previous model with the

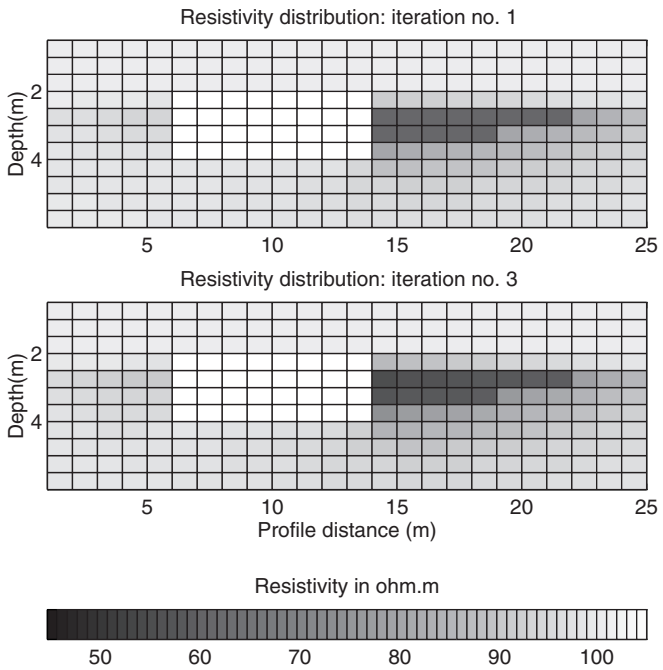

Figure 3. Cross sections given by the solution of the inverse problem after one and three iterations. The scale on the bottom shows the values of resistivity in $\Omega\ \mathrm{m}^{-1}$.

leakage modelled as an additional inclusion of resistivity 20 $\Omega\ \mathrm{m}^{-1}$ near the centre of the right vertical side of the waste container. The size of the leakage is 2.5 m by 1 m by 1 m.

Figure 1 shows a cross section of the models—a real medium with an inclusion which models leakage and a starting initial model with no leakage.

The electric current is assumed to be injected on the surface of the Earth through a set of point electrodes located on a profile going along the long horizontal axes of the container. We assume that each electrode in its turn transmits the current, while all others are the receiving electrodes. We use an integral-equation forward-modelling algorithm [12] in order to calculate the voltage response of the background medium and of the 'real' medium. The accuracy of this algorithm is discussed in [2].

We assume that together with the 'true' voltages the measured data contain some disturbances of rms error equal to ϵ. The eigenvalues $M_1, M_2, \ldots$ which exceed this ϵ correspond to the data containing the information about the inclusion for the given noise level. By neglecting eigenvalues smaller than ϵ, we assure that data rms matching will not be better than ϵ, which is equivalent to contaminating synthetic data with a noise of level ϵ, whose statistical meaning can be specified for the given application.

We find the optimal current distribution on the surface using singular value decomposition of the impedance difference matrix as described in [5]. Figure 2 shows eigenvalues of the problem (9) for this particular conductivity distribution and the surface-current intensity distribution corresponding to the first eigencurrent. We can see that the difference between the first two eigenvalues is quite big, so we can hope to obtain an acceptable inversion result using data of only one optimal current.

Knowing the optimal intensities of the current injected at different electrodes we

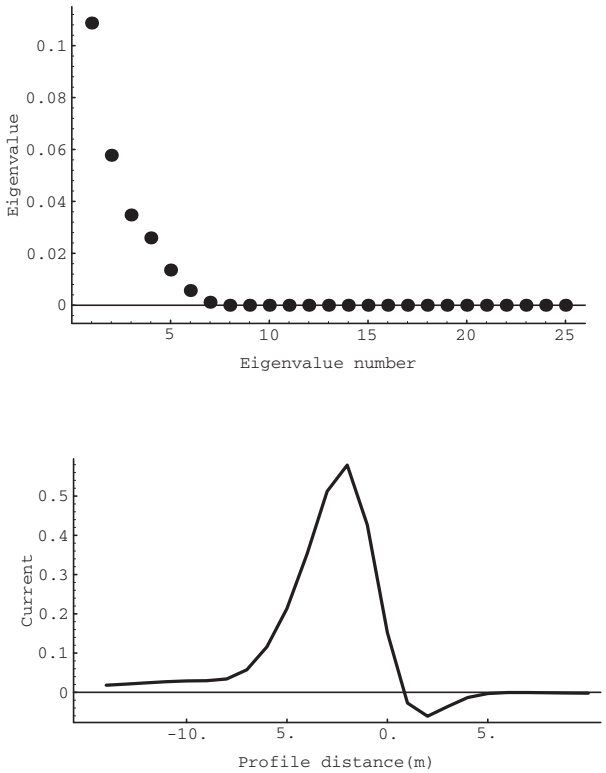

Figure 4. Distribution of eigenvalues M_i after three iterations (top) and the first eigencurrent (bottom).

calculate the optimal background electric field inside the Earth as a weighted combination of the electric fields due to the unit currents. We use a weight function as discussed above to limit the image to features at some depth from the Earth's surface. If the liquid in question is buoyant then this constraint can be changed. The approximate conductivity function σ is proportional to the optimal background electric field. The coefficient of proportionality is calculated as above. This is the first step of the iteration.

In the next step we take the 'improved' conductivity $\gamma + \sigma$ as a background medium γ_1 and repeat the process starting from the calculation of the current distribution which is optimal for distinguishing this new background from the real medium.

Figure 3 shows the cross section of the medium as a result of calculations after one and three iterations.

Figure 4 gives eigenvalues of the impedance difference matrix for the conductivity distribution after three iterations and shows the current intensity distribution corresponding to the first eigencurrent. Comparing the top plot with the eigenvalue distributions in figure 2, we can see a significant decrease of the first eigenvalue, which shows the rms difference between the voltages generated by the real medium and by the medium with conductivity calculated during the described iterative process.

Figure 5 shows the cross section of the medium as a result of calculations after 11 and 23 iterations.

Figure 6 shows the actual difference in voltage data on the surface before starting

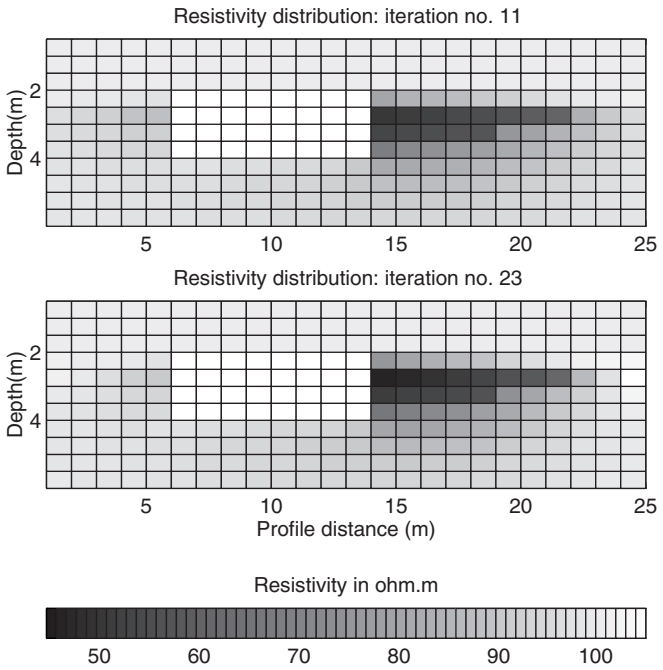

Figure 5. Cross sections given by the solution of the inverse problem after 11 and 23 iterations. The scale on the bottom shows the values of resistivity in Ω m^{-1}.

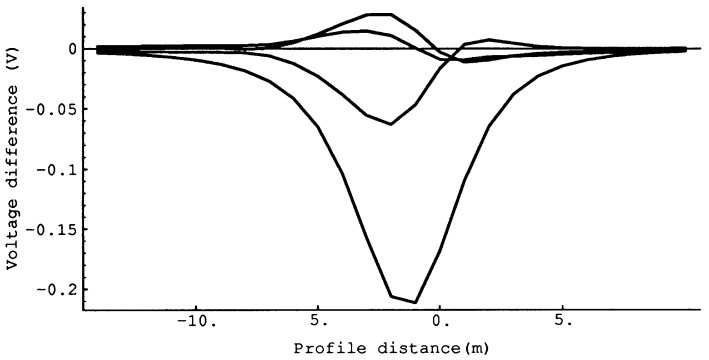

Figure 6. Difference in voltage data on the surface: before starting the inversion and after three, 11, and 23 iterations.

the inversion and after three, 11, and 32 iterations, corresponding to the injection of the currents, optimal for each particular case. Optimality of the injected current guarantees that the observed voltage difference is the maximal possible difference for any applied current possibly generated by the considered system of electrodes.

We can see that even using data of only one current on each iteration, we obtain a reasonable result of interpretation. Of course, the obtained image is not a unique image of the true model, but one of the possible solutions which is close to the true solution for the given noise. Generally, having noise in data of rms error ϵ we can construct an algorithm

taking into account the data generated by the eigencurrents corresponding to the eigenvalues exceeding this level ϵ. This will produce a conductivity distribution which is closer to the true solution, and of course, it will take more computational effort. The algorithm which we used to show the results of computer simulations and which includes only data of one current is the least computationally expensive. On each step it calculates only the forward solution and the electric-field distribution inside the Earth corresponding to the optimal current, avoiding solution of any system of equations.

The advantage of this method is that it is less computationally expensive compared with the methods based on usage of all available data.

8. Conclusion

In the present paper a solution of the inverse electric tomography problem for measurements containing noise is suggested, in which data weights are optimized *vis-à-vis* available *a priori* information at the time of the imaging. The part of the conductivity function σ which is visible from a noise-free experiment is described in [8] as a subspace S of $L^2(\Omega)$ spanned by the functions $\nabla u_i \nabla u_j$. In our notation, S is given by the expression (33).

For measurements containing noise only a part of these projections can be restored. The eigenvalues M_i of the current-to-voltage mapping show what projections of σ can be determined from the data of a given noise level. Hence the space S is naturally presented as a sum of subspaces $T_1 \cup T_2$: the subspace T_1 contains the solution σ, and the subspace T_2 is such that σ is orthogonal to all functions spanning T_2.

The algorithm for constructing an inverse solution for noisy data provides a conductivity function from a set of solutions which are equivalent up to the noise level, hence reducing the problem to an inverse problem of much smaller dimension.

Acknowledgments

We wish to thank Robert V Kohn for helpful discussions and encouragement. This work was supported by DOE/OBES under grant number DE-FG03-93ER14313.

References

[1] Allers A and Santosa F 1991 Stability and resolution analysis of a linearized problem in electrical impedance tomography *Inverse Problems* **7** 515–33

[2] Beasley C W and Ward S H 1986 Three-dimensional mise-a-la-masse modeling applied to mapping fracture zones *Geophysics* **51** 98–113

[3] Bryan K and Vogelius M A computational algorithm for crack determination. The multiple crack case *Preprint*

[4] Cherkaeva E and Tripp A C 1995 Optimal survey design using focused resistivity arrays *IEEE Trans. Geosci. Remote Sens.* **34** 358–66

[5] Cherkaeva E and Tripp A C 1995 On the resolution of geoelectric imaging *SIAM J. Appl. Math.* submitted

[6] Connolly T J and Wall D J N 1988 On inverse problem, with boundary measurements, for the steady state diffusion equation *Inverse Problems* **4** 995–1012

[7] Dobson D C 1992 Estimates on resolution and stabilization for the linearized inverse conductivity problem *Inverse Problems* **8** 71–81

[8] Dobson D C and Santosa F 1994 Resolution and stability analysis of an inverse problem in electrical impedance imaging—dependence on the input current patterns *SIAM J. Appl. Math.* **54** 1542–60

[9] Druskin V 1982 The unique solution of the inverse problem in electrical surveying and electrical well-logging for piecewise-continuous conductivity *Izv., Earth Phys.* **18** 51–3

[10] Gisser D G, Isaacson D and Newell J C 1990 Electric current computed tomography and eigenvalues *SIAM J. Appl. Math.* **50** 1623–4

[11] Harrington R F 1968 *Field Computation by Moment Methods* (New York: Macmillan)
[12] Hohmann G W 1975 Three-dimensional induced-polarization and electromagnetic modeling *Geophysics* **40** 309–24
[13] Isaacson D 1986 Distinguishability of conductivities by electric current computed tomography *IEEE Trans. Med. Imag.* **MI-5** 91–5
[14] Jackson D D 1972 Interpretation of inaccurate, fficient and inconsistent data *Geophys. J. R. Soc.* **28** 97–109
[15] Kohn R V and Vogelius M 1984 Determining conductivity by boundary measurements *Commun. Pure Appl. Math.* **37** 289–98
[16] Narayan S, Dusseault M B and Nobes D C 1994 Inversion techniques applied to resistivity inverse problems *Inverse Problems* **10** 669–86
[17] Parker R L 1977 Understanding inverse theory *Ann. Rev. Earth Planet. Sci.* **5** 35–64
[18] Paulson K, Lionheart W and Pidcock M 1995 POMPUS: an optimized EIT reconstruction algorithm *Inverse Problems* **11** 425–37
[19] Santosa F and Vogelius M 1991 A computational algorithm to determine cracks from electrostatic boundary measurements *Int. J. Engng Sci.* **29** 917–37
[20] Sylvester J and Uhlmann G 1987 A global uniqueness theorem for an inverse boundary value problem *Ann. Math.* **125** 153–69